Nuclear Instruments and Methods in Physics Research A 334 (1993) 229–233
North-Holland

NUCLEAR
INSTRUMENTS
& METHODS
IN PHYSICS
RESEARCH
Section A

Optical filter for X-ray astronomy CCDs

K.-H. Stephan [a], H. Bräuninger [a], C. Reppin [a], H.J. Maier [b], D. Frischke [b], M. Krumrey [c] and P. Müller [c]

[a] *Max-Planck-Institut für Extraterrestrische Physik, W-8046 Garching, Germany*
[b] *Sektion Physik der Ludwig-Maximilians-Universität München, W-8046 Garching, Germany*
[c] *Physikalisch-Technische Bundesanstalt, Institut Berlin, W-1000 Berlin 10, Germany*

Charge coupled device (CCD) detectors are sensitive from the X-ray to the NIR (near infrared) region. For X-ray and soft X-ray observations in astronomy, an optical filter has to be placed in front of the CCD to suppress the UV (ultraviolet) and VIS (visible) radiation of stars by more than 6 orders of magnitude. However, this filter must remain highly transparent at photon energies above 100 eV. A prototype filter was developed for a satellite borne CCD X-ray imaging detector. This unsupported filter has an effective size of 30 mm × 10 mm and is composed of multilayered thin films of parylene N, aluminum and carbon with mass densities of 25, 30 and 25 $\mu g/cm^2$, respectively. The fabrication technique used for the filter and measurements of its optical and mechanical properties are presented.

1. Introduction

The X-ray Multi-Mirror Mission (XMM) is a high throughput spectroscopy mission and the second cornerstone of the ESA (European Space Agency) long term scientific programme [1]. It is now in the electro-optical breadboard (EOBB) phase. The launch into a highly eccentric orbit is planned for the end of the decade.

The X-ray mirror system is being developed under the responsibility of ESA, while the focal plane instrumentation and the optical monitor are being built by consortia under the leadership of the principal investigators. The XMM payload consists of three Wolter-I telescopes with a focal length of 7.5 m having CCD cameras as focal plane instruments for medium resolution spectroscopy with a resolving power between 6 and 60 over the energy range from 0.1 to 10 keV. An optical monitor enables correlated observations in the VIS and UV spectral range. In two telescopes reflective gratings will allow high resolution spectroscopy with a resolving power of 300–400. The total collecting area of the three telescopes, which consist of 58 shell pairs each, is about 6000 cm^2 at 2 keV and about 3000 cm^2 at 6 keV.

The Max-Planck-Institut für Extraterrestrische Physik (MPE) is developing specific pn-Si CCDs optimized for the X-ray band [2]. These CCDs will have high efficiency up to 10 keV, good time resolution and a high radiation hardness. The pixel size is 150 $\mu m \times$ 150 μm, adapted to the angular resolution of the X-ray telescope of about 30 arcsec. Since a very good low energy response is expected with these CCDs due to a thin deadlayer, optimized optical filters are needed to protect the CCDs from ultraviolet and visible radiation.

2. Objective of the work

The quantum efficiency of the CCD is governed by the silicon deadlayer and the depletion depth, which are targeted to have thicknesses of 40 nm and 250 μm, respectively. We calculated the spectral quantum efficiency of the CCD using the optical data from refs. [3,4]. The result shows that the detector is sensitive to radiation from the X-ray to the NIR energy band. The mission profile of the XMM observatory, however, is to observe celestial objects of astrophysical interest in the soft X-ray band.

In orbit very intense UV sources are the geocorona [5] and O, B and A stars [6], the radiation of which must not enter the sensitive CCD surface. For that reason a radiation entrance window having the appropriate filtering characteristics is placed in front of the CCD in order to suppress photons emitted by UV and VIS stars, which are considered as contaminations.

The spectral irradiance in the energy range between 1 and 10 eV of an A1 type star [7] on the CCD surface is expected to be approximately 10^7photons per pixel and integration time. Since less than 10 photons per pixel and integration time are permitted as a background signal, the filter must provide an adequate suppression of the radiation. This will be explained later in more detail.

Based on the optical constants from refs. [3,8–10] we designed a three layered filter composed of parylene N, aluminum, and carbon. Parylene N is opaque in the VUV (vacuum ultraviolet) range and serves as a carrier for a filter without supporting grid. Aluminum is highly opaque in the VIS and NIR range. Carbon defines the cut-off in the VUV range. The thicknesses of the filter constituents are as follows (the corresponding mass densities are given in parentheses):

0.2 μm (25 μg/cm^2) parylene N,
0.1 μm (30 μg/cm^2) aluminum, and
0.1 μm (25 μg/cm^2) carbon.

3. Manufacturing of the filter

A filter sample consists of a sandwich film of three superposed layers of materials as given above, which is mounted on a circular shaped stainless steel frame of 36 mm diameter with an aperture of 10 mm × 30 mm. First, a 25 μg/cm^2 thick parylene N film is condensed by a CVD (chemical vapour deposition) procedure [11] on an optically flat glass substrate which has previously been vacuum coated with a thin, smooth potassium cloride parting agent layer. After deposition of the polymer, the pellicle is floated onto the surface of distilled water, picked up with an annular mount and glued to the sample holder. As a second step, the aluminum film is deposited on the parylene N backing by ion beam sputtering utilizing the xenon beam from a saddlefield ion source [12]. The procedure is conducted in a vacuum chamber with a residual gas pressure of 10^{-6} Pa and a xenon working pressure of 10^{-5} Pa, resulting in a low oxygen content of the aluminum film. Since ion beam sputtering is a cold process, it is well suited for the coating of plastic materials, which are sensitive to heat impingement. Finally, the carbon layer is vacuum condensed on top of the aluminum surface by standard electron beam evaporation techniques at working pressures of 10^{-4} Pa.

The mass densities of the parylene N carrier foil as well as the deposited aluminum and carbon layers were determined by means of a microbalance. The uncertainties of the given layer thicknesses are estimated to be less than ±10%. From elastic recoil detection measurements it is known that Al layers sputter deposited in our facility contain less than 3% oxygen and less than 0.15% nitrogen.

4. Optical properties

4.1. Spectral transmittance

Different facilities were used to determine the spectral transmittance in different spectral ranges.

(1) Soft X-ray range

The measurements were carried out at the 10 m test facility (ZETA) of the MPE [13] in the photon energy range 278 eV < E < 8 keV.

(2) VUV range

The measurements were performed in the radiometry laboratory of the PTB (Physikalisch Technische Bundesanstalt) at the electron storage ring BESSY in Berlin [14]. Synchroton radiation is monochromatized using a toroidal grating monochromator. In principle the photon energy range between 10 and 275 eV is covered by the instrument using a 200 lines/mm grating, but higher orders are present in wide spectral regions. In order to suppress higher order contributions to levels below 2%, two filter wheels are installed behind the exit slit. Suppression is possible in the range between 31 and 275 eV by using thin filters of Mg, Al, Be, and C, and around 10 eV by using a LiF window. To determine the transmission of a filter sample, it is mounted in the measurement chamber on a manipulator arm allowing a two-dimensional scan over the surface to investigate also the homogeneity of the transmittance. By tuning the wavelength in the vicinity of the absorption edges, this procedure is also selective for inhomogeneities of a specific layer material. The beam diameter on the sample can be varied between 0.2 and 2 mm. As a detector either a channel electron multiplier or a GaAsP/Au Schottky diode can be used. A continuous transmission spectrum is obtained as the ratio of two spectra with and without sample in the beam. Depending on the wavelength, the dynamic range covers up to 6 orders of magnitude. The accessible spectral range is being extended towards shorter wavelengths down to 0.8 nm using a plane grating monochromator.

(3) UV range

The investigations were performed in the test facility of the MPE, which was established to measure the quantum efficiencies of the ROSAT imaging focal plane detector [15]. It is comprised of an argon arc [16] serving as a light source which is connected to a 0.5 m Seya Namioka monochromator with an experiment chamber adapted to the exit slit for handling of the filter and detection. A solar blind photomultiplier is used as a detector enabling a dynamic range of up to 6 orders of magnitude in the spectral range between 4.8 and 8.8 eV.

(4) VIS to NIR range

A commercially available spectral photometer (Cary 5) was used at the MPE in the photon energy range between 1.2 and 6.2 eV.

Since the detection limits of the above-mentioned facilities are not significantly lower than 10^{-6} we were

not able to measure the transmittance of the nominal filter below 30 eV. Therefore, we coated parylene N films with thinner layers of aluminum and carbon as follows:

25 $\mu g/cm^2$ parylene N,
25 $\mu g/cm^2$ parylene N + 9.5 $\mu g/cm^2$ Al,
25 $\mu g/cm^2$ parylene N + 25 $\mu g/cm^2$ C.

The transmittance of these samples was measured and the absorptance of the individual constituents derived. Then the transmittance of the nominal filter was calculated. The transmittance above 41 eV was measured on the nominal filter. Below 41 eV the transmittance was derived from the individual samples. A comparison between measured and calculated transmittance of the nominal filter is shown in fig. 1. The numbered ranges refer to the ranges and techniques described above. The six data points shown by open triangles at high energy represent measured transmittances in facility (1) at six discrete photon energies. The data point at 11.2 eV (filled triangle) is derived from measurements at the PTB facility. The data in the other energy regimes are continuous. The solid line (2) was measured in the VUV facility of the PTB. Solid curves (3) and (4) represent the results of measurements in the UV and the VIS to NIR facility, respectively. For comparison with the experimental results the expected spectral transmittance of the nominal filter is shown by the dashed curve (0). It was calculated from published optical data of the components [3,8–10]. The spectral transmittance of the filter features a deep minimum at 12 eV due to the absorption characteristics of parylene N. There is good agreement between experimental and theoretical data in the photon energy range from 41 eV to 10 keV. In the range from 1 to 9 eV the filter

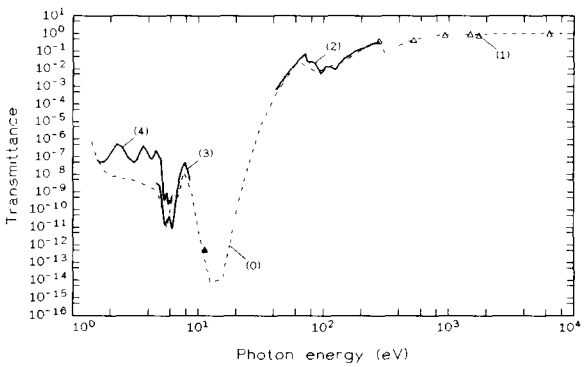

Fig. 1 Transmittance of the XMM/EOBB prototype filter. Comparison between measurement and calculation. Measurements performed at: (1) soft X-ray facility (ZETA) of the MPE/Garching; (2) VUV TGM facility of the PTB at the BESSY storage ring in Berlin; (3) UV facility of the MPE/Garching; (4) spectral photometer (Cary 5) of the MPE/Garching; (0) transmittance calculated from published optical data of the components.

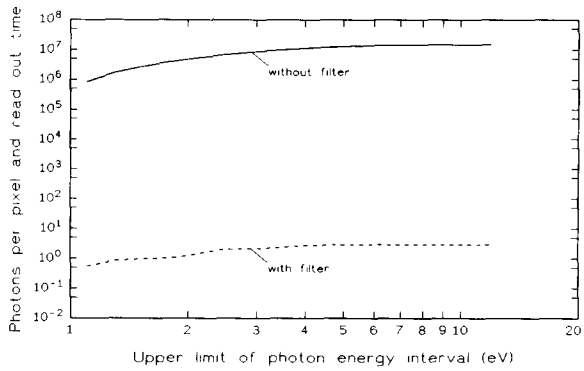

Fig. 2. Number of photons interacting with 1 pixel of the CCD without and with the XMM/EOBB prototype filter. The telescope and CCD performance data are: CCD pixel length $P = 150$ μm; integration time $t = 50$ ms; telescope collecting area $F = 3000$ cm^2; telescope point spread function, PSF = 30 arcsec.

transmittance is up to a factor of 100 higher than expected. The discrepancy can neither be explained by the uncertainties of the measurements, which are less than $\pm 10\%$, nor by the oxygen content of the filters [17].

To estimate the effectiveness of the filter rejecting radiation outside the bandpass of interest, the spectral irradiance on the focal plane CCD surface was calculated as generated by Vega. Since Vega is one of the brightest UV stars, but X-ray dark, sufficient suppression of its visible and UV radiation is a necessary condition for X-ray detectors used in space missions. The mean photon irradiance for one pixel of the CCD due to Vega radiation can be calculated from the spectral photon irradiance at the entrance plane of the telescope and the parameters of the telescope. The incoming photons spread over 50 pixels which have a size of 150 $\mu m \times 150$ μm each. The number of photons incident on a pixel during the integration time of 50 ms is shown in fig. 2 depending on the upper integration limit of the photon energy interval starting at the 1.12 eV bandgap of silicon. Interstellar absorption is not considered. In the energy range between 1.2 and 12 eV, 1.2×10^7 photons per pixel and integration time are obtained without filter in contrast to 3 photons per pixel and integration time with the XMM/EOBB prototype filter.

4.2. Local uniformity of the transmittance

Scans of the local transmittance homogeneity across the filter were caried out with synchroton radiation above and below the Al L_3 absorption edge at 72 eV. The overall uniformity was found to be better than $\pm 2\%$.

4.3. Pinhole density

To estimate the portion of transmitted light due to pinholes an area of 1 cm^2 of the filter was illuminated by a beam at 175 nm in our UV facility producing an irradiance of approximately 10^9 photons/cm^2 s on the filter surface. A solar blind PMT (photomultiplier) used as a detector was located behind the filter. The dynamical range could be extended to 8 orders of magnitude by variation of the amplification factor of the PMT. No statistically significant signals above the detection limit were registered. Thus we conclude that the area fraction of pinholes in the investigated filter is less than 10^{-7}. This result does not allow the estimation of the actual numbers of the pinholes and their individual size. For a first approach we therefore investigated the filter by means of a high resolution microdensitometer (Grant Instruments) and did not detect any pinhole above the detection limit of 0.1 μm in diameter. Whether or not occasional images generated in the detector by pinholes having sizes less than 0.1 μm can be ignored will be subject to further investigations.

5. Environmental tests

The filters must withstand high stresses during the launch phase, and mission in orbit. We tested whether they will be rigid enough to withstand vibration during the first 60 s of the launch as well as the thermal cycles according to the conditions in space. The final layout of the CCD camera is likely to provide a filterwheel which is housed either in an evacuated or a pressurized chamber during the launch phase. For that reason we used a dummy vacuum housing for the environmental tests of the prototype filters.

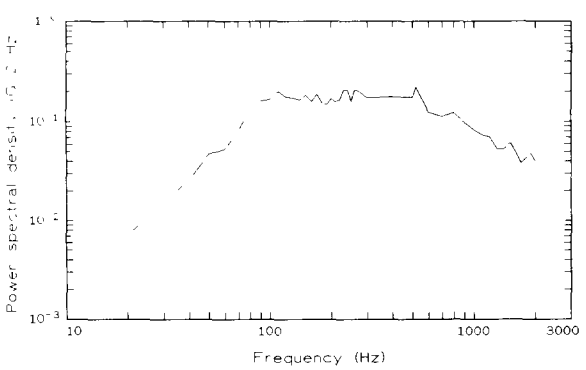

Fig. 3. Sinusoidal vibration testing on the XMM/EOBB prototype filter Duration: 120 s.

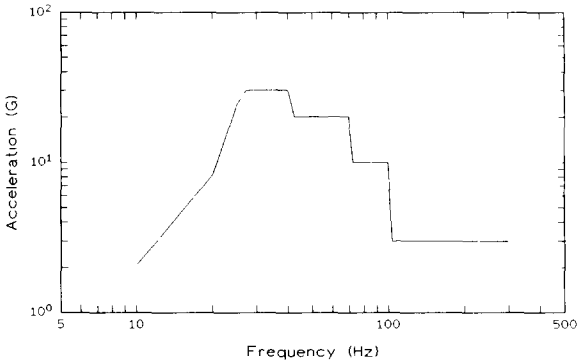

Fig. 4. Random vibration testing on the XMM/EOBB prototype filter. Duration: 120 s.

5.1. Vibration

Five items of filter samples were subjected to random and sinusoidal vibrational loads according to the qualification spectrum provided for ARIANE 4. Figs. 3 and 4 show the power spectral density g^2/Hz for random vibration and the

5.2. Acoustic noise

In the case that the flight model filters will be mounted in a box under vacuum, acoustic noise will be transformed into random vibrational load. The prototype filters housed in the evacuated dummy box passed an acoustic noise test of 120 s duration at OASPL levels of 139 dB [18] and did not show any defects afterwards.

5.3. Thermal stress

To simulate the thermal conditions during storage, operation and annealing of the CCD the filter was subjected to a thermal load cycle corresponding to temperatures of $120 \leqslant T \leqslant 320$ K during a period of 2 h. No damage was observed to the filters.

6. Conclusion

We have fabricated and tested a multilayered thin film composition to study the feasibility of optical filters in front of a satellite borne CCD X-ray imaging detector. A prototype filter proved to be sufficiently stable when subjected to the required environmental stresses. We achieved the design goal of suppressing radiation in the range 1–25 eV by more than 6 orders of magnitude. However, the discrepancies between expected and measured transmittances at photon energies below 9 eV need an explanation. To achieve better

agreement between measurements and theoretical predictions it is helpful to combine transmittance measurements and data from analysis of the constituents and perform model fits. We previously applied this method successfully for the analysis of ROSAT-boron filters [19]. Based on the described experiences, we feel encouraged to develop a concept for unsupported large area flight model filters for the XMM mission profile, which may be optimized for different bandpasses. At present we are going to establish an ultra high vacuum facility for thin film deposition using cold and hot processes. The final flight model filters require an effective size of 60 mm in diameter not supported by a mesh. At present a filter wheel for adaptation of several filters is under construction. Filters having different bandpass characteristics and cut-offs in the range from 10 to 100 eV are being considered.

Acknowledgement

We wish to express our thanks to Dr. W. Assmann, who determined the oxygen and nitrogen contents of the aluminum films by heavy ion elastic recoil detection (HIERD) techniques.

References

[1] P.L. Jensen, J.M. Ellwood and A. Peacock, ESLAB Report 89/91 (1989) p. 1.
[2] H. Bräuninger et al., EUV, X-ray, and gamma-ray Instrumentation for Astronomy II, SPIE 1344 (1990) 330.
[3] B.L. Henke et al., At. Data Nucl. Tables 27 (1986) 1.
[4] S. Labov, S. Boyer and G. Steele, Appl. Opt. 24 (1985) 576.
[5] R. Huffman et al., J. Geophys. Res. 85 (1980) 2201.
[6] ESA SR-28, Supplement to the Ultraviolet Bright Star Spectrophotometric Catalogue (1978).
[7] M.V. Zombeck, Handbook of Space Astronomy and Astrophysics (Cambridge University Press, Cambridge, 1982) p. 60.
[8] H.J. Hagemann, W. Gudat and C. Kunz, Optical constants from the far infrared to the X-ray region, DESY SR-74/7 (1974) 1.
[9] R. Stern and F. Paresce, J. Opt. Soc. Am. 65 (1975) 1515.
[10] H. Kaase and K.-H. Stephan, Internal report PTB-Braunschweig, Labor 4.14 (1982) p. 1.
[11] W.F. Gorham, J. Polymer Sci. 4 (1966) 3027.
[12] H.J. Maier, Nucl. Instr. and Meth. A303 (1991) 172.
[13] B. Aschenbach, H. Bräuninger, K.-H. Stephan and J. Trümper, Space Optics-Imaging X-ray Optics Workshop, SPIE 184 (1979) 234.
[14] M. Krumrey, M. Kühne, P. Müller and F. Scholze, Multilayer Optics for Advanced X-Ray Applications, SPIE 1547 (1991) 136.
[15] H. Kaase and K.-H. Stephan, Appl. Opt. 18 (1979) 2275.
[16] J.M. Bridges and W.R. Ott, Appl. Opt. 16 (1977) 367.
[17] F. Powell, X-Ray Instrumentation, SPIE 1140 (1988) 88.
[18] Bericht Nr. B-TA 3130, Industrieanlagen-Betriebsgesellschaft mbH D-8012 Ottobrunn (1992) p. 14.
[19] K.-H. Stephan, J.H.M.M. Schmitt, S.L. Snowdon, H.J. Maier and D. Frischke, Nucl. Instr. and Meth. A303 (1991) 196.